

# On-chip technologies for multidimensional separations†

Samuel Tia and Amy E. Herr\*

Received 12th January 2009, Accepted 2nd March 2009

First published as an Advance Article on the web 23rd March 2009

DOI: 10.1039/b900683b

We review microfluidic devices designed for multidimensional sample analysis, with a primer on relevant theory, an emphasis on protein analysis, and an eye towards future improvements and challenges to the field. Image shows results of an on-chip IEF-CE separation of a protein mixture; unpublished surface plot data from A. E. Herr.

## 1. Introduction

While systems biology and proteomics are powerful paradigms for biological studies, further advances hinge on breakthroughs in bioanalytical technologies. As early as the 1950's, researchers identified the need to increase the number of species analyzed in a single assay over available one-dimensional (1D) analysis. Tools for 1D analysis can separate biomolecules based on a single physical or chemical property such as size, charge or affinity. Analytical chemists looked to two-dimensional (2D) and multidimensional separations to increase the analysis capacity of assay systems.<sup>1</sup> In 1984, Giddings aptly noted that "2D technology must stand on the shoulders of 1D building blocks".<sup>2</sup> Regardless of format – slab gel, capillary, or microchip – multidimensional assays require systems design and integration considerations to yield performance improvements over 1D assays.

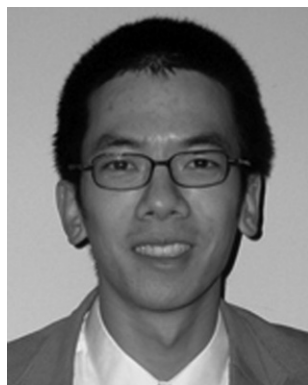
Developers of multidimensional separations work to optimize the performance of combined assays, most critically the rela-

tionship between the respective separation mechanisms and the transfer of sample between assays. A primary aspect of multidimensional assay development is the compatibility of the separation dimensions, specifically the orthogonality (or independence) of the individual dimensions when implemented in tandem. A myriad of chromatographic and electrophoretic approaches, including high pressure liquid chromatography (HPLC), isoelectric focusing (IEF), and sodium dodecyl sulfate polyacrylamide gel electrophoresis (SDS-PAGE), have been combined in various ways to improve and optimize the information available from a single assay.<sup>3–9</sup> The number of useful assay combinations increases when mass spectrometry (MS), which aids in identifying the chemical composition of a sample based upon the mass-to-charge ratio of its constituent species, is added as an analysis dimension.<sup>10–12</sup> Further, developers of 2D separations seek to surmount daunting challenges in control of the physicochemical interface between the dimensions. Special attention is paid to performance-degrading dispersion which corrupts sampling efficiency and effectiveness.

In this review, we consider microfluidic systems as one possible technology for addressing challenges in the coupling of independent 1D separations. We focus on microfluidic multidimensional protein separations developed over the previous ten years. First we present a primer on the rationale behind multidimensional

Department of Bioengineering, University of California, Berkeley, 308B Stanley Hall, MC # 1762 Berkeley, CA, 94720-1762, USA. E-mail: AEH@BERKELEY.EDU

† Part of a *Lab on a Chip* themed issue on fundamental principles and techniques in microfluidics, edited by Juan Santiago and Chuan-Hua Chen.



Samuel Tia

Samuel Tia is an NSF research fellow and PhD student within the Joint Graduate Group in Bioengineering at the University of California Berkeley and UC San Francisco. Prior to his doctoral studies at the University of California, he graduated from the University of Florida with a B.S. degree in Mechanical Engineering.



Amy E. Herr

Amy E. Herr is an Assistant Professor at the University of California, Berkeley affiliated with the Joint Graduate Group in Bioengineering (UC Berkeley and UC San Francisco) and a faculty scientist at Lawrence Berkeley National Laboratory (Physical Biosciences Division). She completed her B.S. in Engineering & Applied Science at the California Institute of Technology, and her M.S. and Ph.D. degrees in Mechanical Engineering at Stanford

University. In 2007, after holding a staff scientist position at Sandia National Laboratories, she joined the faculty in Bioengineering at UC Berkeley.

separations, followed by detailed descriptions of specific strategies used in device design, fabrication, sample injection, data collection and analysis for microfluidic multidimensional separations. We highlight fundamental performance measures required of multidimensional separations, review recent microfluidic approaches to achieving said performance, and look to the future by discussing the promise and challenges facing microfluidic multidimensional systems.

## 2. Rationale for microfluidic multidimensional separations

### System performance

For both single-dimension and multidimension assays, there are several key performance metrics.<sup>15</sup> Separation resolution,  $SR$ , is defined as the ratio of the distance between neighboring sample peaks to the width of a sample zone:

$$SR = \frac{\Delta L}{4\sigma} \quad (1)$$

Here,  $\Delta L$  is the center-to-center distance between peaks (or zones) of interest and  $4\sigma$  is the average width value for the two analyte bands under consideration.  $SR$  can be thought of as the peak-to-peak distance between neighboring zones normalized by the average zone width. In separations of multiple analytes, the overall separation resolution is the  $SR$  for the two analytes which are most difficult to separate.  $SR$  is a critical factor in characterizing the efficiency of a separation. Dispersion, or band broadening, reduces  $SR$ . Sample broadening may result from the following sources: molecular diffusion, dispersion arising from the injection, turn-induced dispersion, pressure gradient-induced dispersion, Joule-heating-induced dispersion, and the size of the detection region. In addition to  $SR$ , the analytical detection sensitivity plays a key role in defining separation performance. Choice of detector location,  $L_d$ , is dictated by a trade-off in maximizing  $SR$  while maintaining sufficient detector sensitivity (*i.e.*, signal-to-noise ratio).

One metric that is common for evaluating separation performance is the theoretical plate height ( $H$ ) and its derivative measure, the number of theoretical plates ( $N_t$ ). These are defined as:

$$H = \frac{\sigma^2}{L_d} \quad (2)$$

and

$$N_t = \left(\frac{L_d}{\sigma}\right)^2 \quad (3)$$

Increased  $N_t$  correlates with improved separation efficiency, with the inverse being true for  $H$ . Bharadwaj *et al.* have proposed that  $SR$  combined with an evaluation of the signal to noise ratio (SNR) serve as the best measures of performance for on-chip separation systems.<sup>13</sup> The SNR is defined as the signal peak height divided by the standard deviation of the background signal.

A performance metric often employed for multidimensional separations is the total peak capacity,  $n_{total}$ , of the separation

system. In a single dimension, the peak capacity is defined as the maximum number of separated peaks contained per unit separation length for a selected critical  $SR$ , denoted here as  $SR_{crit}$  (often  $SR_{crit} \sim 1$ ). For a given separation length,  $L_c$ , the peak capacity ( $n_c$ ) for an isocratic separation is given by:

$$n_c = \frac{L_c}{4\sigma \cdot SR_{crit}} \quad (4)$$

In the case of a gradient elution process, the peak capacity must be adjusted to:

$$n_c = 1 + \frac{t_g}{W} \quad (5)$$

where  $t_g$  is the gradient time and  $W$  represents the peak width.<sup>14</sup> For a multidimensional system, the total peak capacity is maximally a multiplicative product of the capacities from each 1D mode,  $n_i$ , brought together in an  $n$ th-order separation:<sup>15</sup>

$$n_{total} = \prod_{i=1}^n n_i \quad (6)$$

This formulation highlights the potential separation power available from a multidimensional approach, assuming that the utilized modes of separation are completely orthogonal to one another. The selection of orthogonal mechanisms to achieve a high total peak capacity is critical when one considers the high probability of peak overlap when dealing with complex samples. For a sample containing  $m$  components undergoing a separation mechanism with a peak capacity  $n_c$ , it can be statistically demonstrated<sup>15</sup> that the number of components which can be resolved as single peaks ( $s$ ) is given by:

$$s = m \exp\left(-\frac{2m}{n_c}\right) \quad (7)$$

Thus for a sample containing 100 components, within a separation system with a peak capacity of 200, it is likely that only 37% of total components will be singly resolved. For the effective separation of a biological sample containing a high number of components, it becomes clear that  $n_c$  needs to be much higher than  $m$ .

To yield maximal information about each analyte, multidimensional combination strategies typically include two different modes of separation although three<sup>16</sup> and even four dimensional<sup>17</sup> separation systems are possible, often when MS is included. Indeed, the inclusion of MS tools becomes a powerful asset when bottom-up “shotgun” proteomic analyses are utilized.<sup>18–22</sup> Multidimensional separations have been performed on various mediums including slab gels,<sup>1,8,23–25</sup> glass capillary tubes,<sup>4,6,7,9</sup> or within chromatographic columns such as in HPLC.<sup>3,21,22,26–30</sup> Specific applications for multidimensional separations include the analysis of oligomers,<sup>26,28</sup> metabolites<sup>31,32</sup> and proteins.<sup>24,33</sup> Reviews by Cooper *et al.*, Fournier *et al.*, Issaq *et al.* and Neverova and Van Eyk provide excellent detail on previous work involving MS.<sup>19,34–36</sup>

### Sampling strategies

Both “heart cutting” and “comprehensive” sampling techniques, as well as spatially-multiplexed and time-multiplexed methods are used to sample species into successive separation dimensions.

“Heart cutting” methods sample one discrete zone from the first dimension into the second.<sup>37–41</sup> The “heart cutting” technique is useful to obtain high separation resolution for a single fused peak from the first dimension. In the comprehensive approach, sequential aliquots from the first dimension effluent are sampled into the second separation dimension, making the method applicable to analysis of all species including multiple fused peaks.<sup>42–46</sup> Optimized sampling parameters developed by Murphy and colleagues for the comprehensive approach suggest that the second dimension separation should be significantly faster than that of the first dimension.<sup>47</sup> The comprehensive sampling approach is often automated and issues of over-sampling and under-sampling are critical. Sampling into a subsequent dimension is similar to the discretization of an analog signal, as under-sampling can result in a loss of information within the final proteomic profile. To achieve the highest possible resolution, each peak from the first dimension must be sampled at least three times into the second dimension when the sampling is in phase (synchronized to the arrival of the eluting band).<sup>47</sup> For a maximally out of phase sampling process, at least four samples per peak are necessary to ensure that all eluting compounds are brought into the second dimension. A consideration of the narrowest peak of interest in the first dimension helps to determine the sampling rates for each multidimensional time-multiplexed separation. Relative assay speed constraints arising from the comprehensive approach limit the types of assays suitable for coupling in this manner.

### Realizing microfluidic multidimensional assays

Because of the diversity of proteins and the seven to twelve orders of magnitude<sup>48</sup> expression range found in biological fluids, adaptable technologies that provide high-resolution and high dynamic range detection are critical tools for proteomic research. To meet performance challenges, researchers are focusing attention and effort on development of multidimensional separations using microfluidic technologies. Interest in microfluidic tools stems from critical performance advantages afforded through use of microsystems. Most relevant to multidimensional separations are advantages in improved throughput due to rapid separation abilities at the microscale, low sample volume requirements, and perhaps most importantly, the integration of functions. In this review, we consider microfluidic systems in which the most significant stages of analysis, including multimodal separation and specimen transfer are integrated into a monolithic device.<sup>49</sup> Previous literature includes review of microchip technologies coupled with off-chip analytical systems, including MS and capillary-based chromatography, which we do not cover here.<sup>18,50</sup>

The choice of a proper substrate material is critical in the design of microscale separation devices. One must consider factors such as ease of fabrication, optical properties and biocompatibility. Perhaps the earliest microfabricated device intended for multidimensional separation was fabricated from fused quartz and reported by Becker *et al.*<sup>51</sup> in 1998. The chip design demonstrated the possibility of two-dimensional capillary electrophoresis based on an intersecting array of 500 parallel microchannels. Borosilicate glass is another similar material with excellent optical properties that is commonly used in device fabrication. Glass and quartz both generate minimal background

fluorescence from the channel substrate which can limit the attainable detection sensitivity. Silicon devices are typically fabricated through standard lithographical techniques that were developed in the semiconductor industry,<sup>52,53</sup> though micro-milling processes may be utilized as well.<sup>54,55</sup> Facile adaptation of conventional silicon fabrication methods in conjunction with the rigid modulus of elasticity and dependable bonding properties resulted in use of silicon as a common material in early microfluidics work.

More recently, polymers have been used, including: poly(dimethylsiloxane) (PDMS), poly(methylmethacrylate) (PMMA), and polycarbonate. Polymeric substrates are generally less delicate than glass devices and are relatively easy to machine, as well as potentially inexpensive when produced in mass. PMMA is a non-conducting material with high dielectric strength which serves as the substrate of choice in the majority of microdevices for multidimensional separation reviewed here. While other polymeric materials have been demonstrated to adversely influence the formation of polyacrylamide gels, PMMA will not interfere with gel polymerization.<sup>37</sup> Although the micromilling techniques used with PMMA are fairly versatile, these techniques are still quite sensitive to vibration and variations in machining parameters. Thus, fabrication methods such as laser ablation,<sup>56–59</sup> plasma etching<sup>60,61</sup> hot embossing<sup>62,63</sup> and injection molding<sup>64</sup> are also common, especially for high throughput manufacturing applications. The glass, silicon and polymeric materials discussed here are frequently used in biomolecular research applications. However, to varying degrees, these material surfaces may experience nonspecific protein adsorption which can result in significant amounts of sample loss and have a negative effect on experimental repeatability. In many cases, surface modifications to the material are necessary to minimize analyte adsorption to microchannel walls.<sup>65</sup>

### 3. Coupled modes of separation benefit from microfluidic technology

In this section, we review demonstrated multidimensional separations developed on microfluidic platforms. We begin with some of the earliest work in on-chip multidimensional separations, which utilized micellar electrokinetic chromatography (MEKC) and microchip capillary electrophoresis (CE). Next, an overview of microdevices for combined isoelectric focusing and electrophoresis for the analysis of proteins is presented along with discussion of relevant techniques employed to improve resolution and ease of use. Finally, alternative modes for performing multidimensional separations within a microfluidic device will be reviewed. To achieve the highest possible peak capacities and to ensure an accurate estimate of  $n_{total}$ , each of the coupled modes of analyte separation presented below were chosen based on a demonstrated mechanistic independence.

#### Micellar electrokinetic chromatography – electrophoresis

MEKC allows charge neutral species to be separated in an electric field, and expands both the scope and sensitivity of conventional electrophoresis. Through MEKC, species are separated based upon differential partitioning between a pseudo-stationary micellar phase and an aqueous mobile phase.<sup>66</sup>

Electrophoresis separates analytes on the basis of charge-to-mass differences (*i.e.*, electrophoretic mobility). By building upon methodologies established for microfluidic MEKC<sup>67–69</sup> and adding in a time-multiplexed CE separation in a second dimension microchannel, the Ramsey group demonstrated one of the first 2D separations on-chip.<sup>44,45</sup> In developing the 2D system, the group tackled the performance degrading problem of geometry induced dispersion at microchannel turns. As with electrophoretic and chromatographic assays in general, the separation length,  $L_d$ , directly impacts the attainable  $SR$  for MEKC.<sup>15</sup> Consequently, in order to achieve the highest possible  $SR$  within the smallest device footprint, serpentine microchannel geometries have been used. The serpentine channel network provides an increased channel length per unit chip area.

Typically, the inclusion of turns results in a broadening of the analyte band owing to turn-induced dispersion arising in part from the “racetrack” effect.<sup>70</sup> Owing to this racetrack effect, charged analyte molecules migrating along the channel length (axial transport) cover less linear distance if following path lines closest to the interior radius of a turn.<sup>71–73</sup> Compounding the effect, the field strength is higher along the shorter path length, thus causing the analyte molecules on the inside of the turn to migrate with an even higher velocity. Researchers have characterized turn-induced dispersion through mathematical models, numerical simulation, and empirical observation.<sup>74,75</sup> Proposed dispersion-reducing methods include altered channel geometries and the inclusion of compensating pairs of turns in opposing directions.<sup>74–76</sup> In the MEKC-CE microdevice system, Ramsey and co-workers introduce tapered asymmetries at the turns, which reduces turn-induced variance, resulting in an increased

peak capacity.<sup>44</sup> Using single point detection, electropherograms were generated for both the MEKC and CE separation dimensions (Fig. 1). The MEKC-CE approach resolved fluorescently labeled tryptic digests in glass microchannels, with total peak capacities as high as 4200.<sup>44</sup> The assay was also used for analysis of chicken egg ovalbumin and bovine serum albumin (BSA), among other proteins.

In other work, Shadpour and Soper integrated MEKC and microcapillary gel electrophoresis (CGE) on a single PMMA device, achieving a peak capacity of 1121.<sup>46</sup> SDS was introduced as a denaturing agent in the gel electrophoresis dimension. In a unique set-up, gel electrophoresis served as the first dimension of separation before the analyte was repetitively transferred into a 10 mm MEKC separation channel. The CGE-MEKC sequence was chosen because MEKC separations were significantly faster than the SDS microchip CGE separations. This gel sieving matrix for CGE reduced the band diffusion that occurs in comparison to free solution MEKC, which helped maintain tight band widths and maximum resolution when first dimensional species were parked for sampling. The authors employed a comprehensive data collection technique; sampling of analyte from the first dimension into the second dimension was carefully controlled by current or voltage control *via* a programmable multi-channel high power voltage supply. In this manner, the electrokinetic direction of flow was diverted through “gates” which opened and closed to control sampling into the second dimension. Peak capacity in the CGE separation was 19, while that of the MEKC dimension was 59. In the analysis of a mixture of ten different proteins, the  $SR$  was calculated to be 2.8 and 4.9 for the CGE and MEKC separations, respectively.

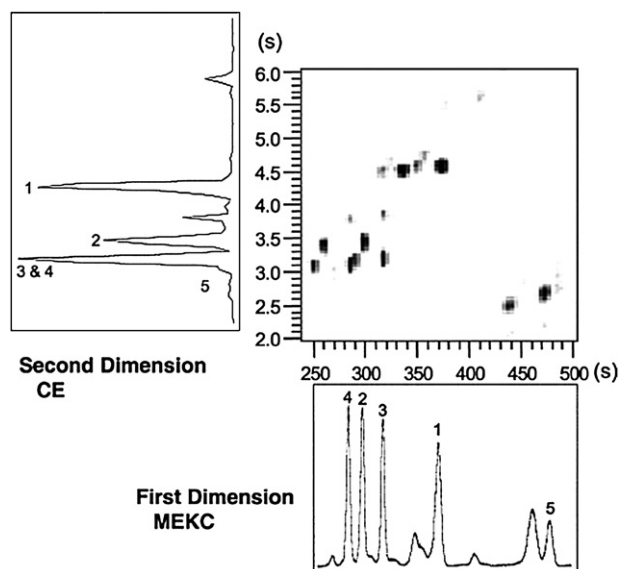


**Fig. 1** Electropherograms from 1D separations of FITC-labeled peptide standards are compiled and displayed as a 2D plot. Every 4 s, effluent from the first dimension is injected into the second. The identifiable labeled peaks correspond to: (1) leucine enkephalin, (2) angiotensin I, (3) angiotensin III, (4) neurotensin, (5) bradykinin. Buffers were 50 mM TEA, 25 mM acetic acid, pH 10.7, with 10 mM SDS (MEKC) and without SDS (CE, bottom). Reprinted with permission from Rocklin *et al.*<sup>45</sup> Copyright 2000 American Chemical Society.

### Isoelectric focusing – electrophoresis

By far, the largest body of work in on-chip multidimensional separations has been with the goal of creating a highly efficient microchip analogue to slab gel two dimensional polyacrylamide gel electrophoresis (2D PAGE). 2D PAGE analogues are comprised of isoelectric focusing and electrophoresis. The IEF dimension is based on the relationship between the charge of a molecule (isoelectric point) and the pH of the surrounding buffer. By establishing a pH gradient in the first dimension and running electrophoresis in the second, 2D PAGE systems are capable of resolving proteins according to isoelectric point and molecular weight (*i.e.*, size).<sup>8</sup> The slab gel 2D PAGE format currently serves as the gold standard for multidimensional separations of most proteins, being readily accessible and having peak capacities on the order of 3000–5000.<sup>8,77</sup> However, slab gel implementations typically require a substantial run time (hours) and can be painstakingly laborious.<sup>78</sup>

Microchip IEF-CE systems have been optimized to achieve separations within less than ten minutes, a dramatic reduction of two orders of magnitude when compared to the time necessary to complete 2D slab gel PAGE.<sup>39</sup> Variations abound, with implementations that employ denaturing SDS treatment<sup>37–40,54,79–81</sup> (which eliminates the variability in the charge-to-mass ratio of proteins), as well as versions that do not employ SDS.<sup>43,82</sup> IEF-CE in microdevices is often implemented using a spatially-multiplexed technique.<sup>54,79–82</sup> On-chip IEF-CE can be performed most simply with two intersecting channels<sup>41,43</sup> or with an array

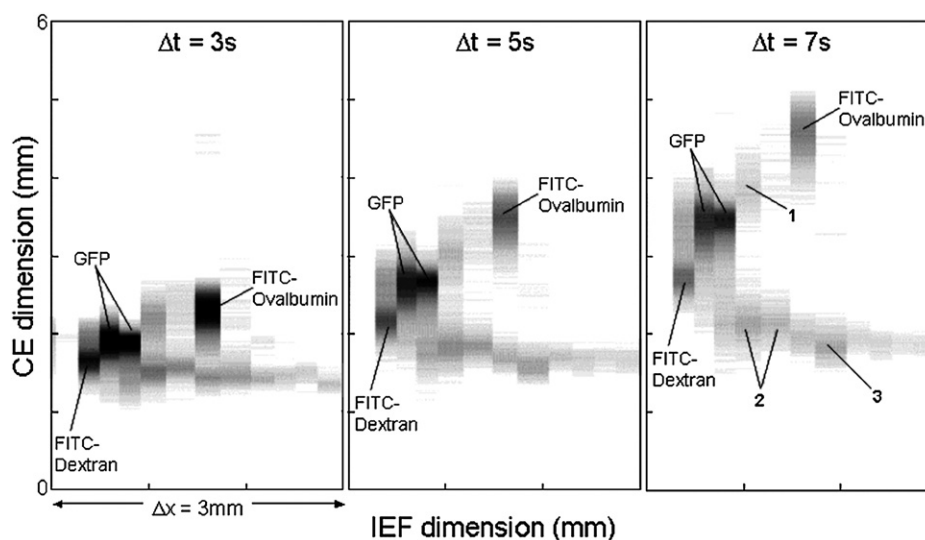


**Fig. 2** Gel-like plots of an IEF-CE separation are displayed for CE analysis times of 3, 5, and 7 s, demonstrating that the center of mass of each identifiable species moves linearly as a function of time. The horizontal axis corresponds to the relative position of each fluid element during the IEF separation, while the vertical axis corresponds to the spatial axial dimension of the subsequent CE separations ( $E = 390 \text{ V/cm}$ ). Approximately 3 mm, or 15%, of the total IEF channel length was sampled ( $E = 350 \text{ V/cm}$ ). Species not identified in companion 1D separations are labeled as peaks 1, 2, and 3. Reproduced with permission from Herr *et al.*<sup>43</sup> Copyright 2003 American Chemical Society.

of parallel second dimension channels intersecting a single first dimension channel.<sup>54,79–82</sup> In early work, Herr *et al.*<sup>43</sup> demonstrated the possibility of 2D IEF-CE on a PMMA microchip with microchannel IEF coupled to free solution capillary electrophoresis in the second dimension at a single cross channel. The 2D separation technique offered enhanced species resolution when compared to independent 1D techniques, as anticipated from multidimensional separation theory (see peaks marked 1, 2, 3 in Fig. 2). The estimated peak capacity of 1300 was limited by the spatial resolution of the sampling junction (with a capacity of  $\sim 130$  in the IEF direction and  $\sim 10$  for the CE separation).

**Modular systems.** Two key dispersion-inducing challenges can arise at the physicochemical interface of two separation dimensions: geometry-associated injection dispersion and injection dispersion arising from heterogeneous buffer systems (*i.e.*, instabilities<sup>83,84</sup>). In spatially-multiplexed systems, geometry-associated injection dispersion often occurs while the analyte is parked in the first dimension. An approach taken by the Whitesides group in an attempt to reduce this diffusion at open-channel intersections utilized a modular PDMS valve system to physically isolate orthogonal microchannels from each other.<sup>39</sup> Here, the authors used a modular strategy in which a single IEF channel was coupled with 100 capillaries used for electrophoresis. PDMS layers were stacked in a multilevel three dimensional configuration and manually rearranged according to the separation stage. In this manner, the intersections between various modes of separation were not in physical contact until just before sample transfer became necessary. Due to the small dimensions of the features on the PDMS layers, the placement of each level was carefully aligned under a microscope. During coupling of the IEF separation with the multiple CE capillaries, lateral non-uniform gaps sometimes resulted at the point of sample transfer. Further optimization of the interface may

alleviate resolution-reducing dispersion arising from the non-ideal geometry.

A more recent paper by Demianova *et al.* adopted a similar modular strategy for combined 2D electrophoresis.<sup>37</sup> PMMA layers with integrated electrodes were stacked, disassembled and realigned for each separation process. The major difference between the modular Demianova *et al.* approach and the modular approach used by the Whitesides group was that instead of transferring proteins from IEF to an array of channels for CE, proteins were electrophoretically transferred from the IEF separation into a prepared miniaturized slab gel. Griebel and colleagues also utilized a modular approach to meet the challenge of developing immobilized pH gradients for IEF. In the work, the authors demonstrated improved reproducibility of IEF separations by designing a credit card sized device in PMMA which accepts a prepared immobilized pH gradient (IPG) strip.<sup>38</sup> The IPG strips, which could be prepared in advance, dehydrated and then stored for several months at  $-20^\circ\text{C}$ , provided a flexible and reusable media for the first dimension of separation. A transfer channel at the interface to 300 parallel microchannels added the possibility of SDS-treatment of the proteins for gel electrophoresis. Finally, a programmable array of integrated electrodes helped provide an optimal (highly focused with narrow bands) protein distribution without peak tailing.

Usui *et al.* also incorporated a commercially available IPG strip into the design of a PMMA device.<sup>40</sup> A special “junction structure” was designed as a valveless interface to connect and separate the first dimensional IPG strip from the second dimensional separation, which took place within an on-chip miniature slab polyacrylamide gel. The device also utilized capillary action at a sample introduction port to prevent solution leakage. All major steps of the two dimensional separation were performed without relocating any components of the chip system in the middle of the process. More than 100 protein spots from

tissue (*i.e.*, Cy5-labeled lysate from mouse brain) were separated and visualized using full-field CCD imaging.

**Dispersion control strategies.** Tsai *et al.* designed an air-gap capillary in a glass device at the junction between the first dimension IEF channel and the second dimensional parallel array of 11 microchannels.<sup>54</sup> The 2-mm wide air gap prevented contamination between the first and second dimension channels during IEF. After the IEF step was completed, the gap was filled with electrophoresis run buffer. Thus the air-gap functioned to temporarily decouple the two separation dimensions. In practice however, fluid and contamination control at the air-gap capillary was somewhat problematic.

Das and coworkers offered an alternative solution to the interfacing problem by placing photopolymerized pseudo-valves of polyacrylamide gel within a polymer device at the regions of channel intersection.<sup>79,85</sup> *In situ* photoinitiated cross-linked gels have been well-documented for microchannel separations,<sup>86–92</sup> and here the technique was used to form a barrier to prevent diffusion while simultaneously allowing the passage of charge carrying proteins. The presence of the polyacrylamide barriers had no effect on IEF behavior while simultaneously increasing the resolution of a BSA/ovalbumin separation as compared to other devices. In a similar fashion, Liu *et al.* used *in situ* photopolymerized polyacrylamide gel plugs as a means to separate two different separation media in a PMMA chip.<sup>81</sup> The ampholyte

mixture in the IEF direction was prevented from leaking into the second dimension, comprised of CE channels. Gel plugs provide the ability to introduce different separation media and customize the composition of the sieving gel for specific applications. Repeatable data collection was demonstrated using FITC-labeled lysate of *E. coli* as a model sample.

Emrich *et al.* have tackled the interface problem in IEF-CE by designing a microfluidic geometry to minimize the diffusion that occurs at junctions between dimensions (Fig. 3).<sup>82</sup> At the junction, interface channels were 25  $\mu\text{m}$  wide, with a total cross-sectional area 65 times smaller than that of the separation channels. By keeping the gel loading channels small and arranging each second dimensional separation channel at a constant length, the authors were able to ensure uniform gel loading and equal resistance (both electrical and fluidic) across every electrophoretic separation channel. The microfluidic multidimensional separation was used to reproducibly observe increased levels of protein expression over successive time points. Adopting a differential in-gel electrophoresis approach, the authors used Cy2 and Cy3 labeled pooled lysates of *E. coli*, following induced expression of maltose binding protein. An estimated capacity of 48 was achieved in the IEF direction, and the combined analyses could be performed at cell lysate concentrations as low as  $\sim 100$  ng/ $\mu\text{L}$ , which represents the contents of approximately 440,000 cells.

The Han group utilized active polymeric valves as a means to separate buffer and sample solutions in a PDMS microdevice.<sup>41</sup> Integrated pressure actuated valves for microdevices are frequently fabricated and used within layers of soft elastomers

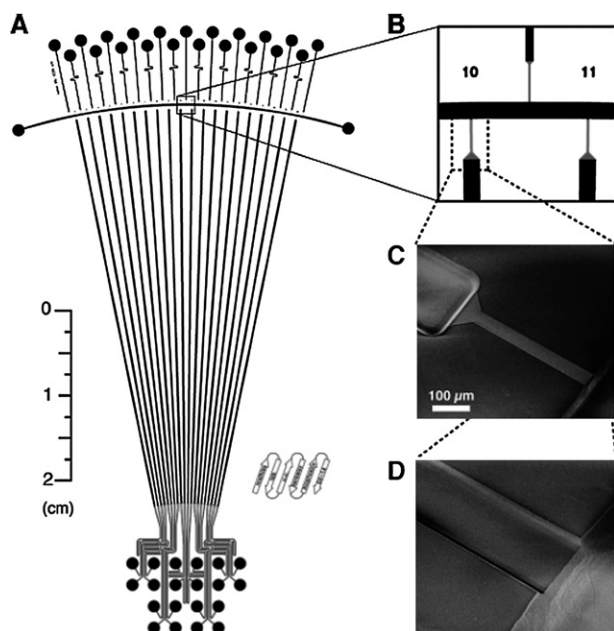


**Fig. 3** A micro-DIGE device enables high resolution protein analysis. (A) The overall design comprises an arced, 3.75 cm long horizontal channel for first dimension isoelectric focusing (IEF) that is punctuated with 20 6.8 cm long vertical channels through which focused proteins are separated in the second dimension by native gel electrophoresis. (B) The separation channels of the two dimensions are joined by much smaller channels forming a microfluidic interface (MFI) that fluidically decouples the contents of the two separation dimensions, seen more clearly in electron micrographs (C and D). The MFI channels are 25  $\mu\text{m}$  wide, 400  $\mu\text{m}$  long, and are etched 4  $\mu\text{m}$  deep. Reproduced with permission from Emrich *et al.*<sup>82</sup> Copyright 2007 American Chemical Society.

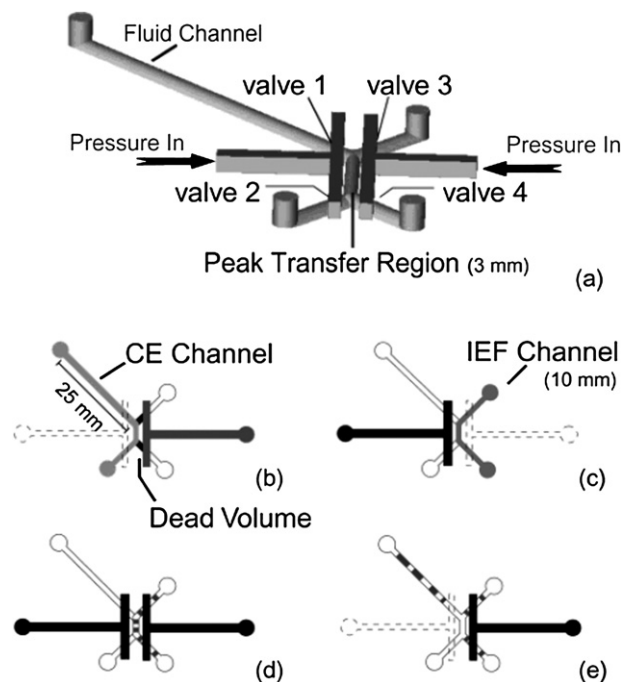


**Fig. 4** The double layer PDMS channel is actively engaged through four distinct stages of separation: (a) perspective view; (b) CE buffer loading; (c) IEF ampholyte mixture loading; (d) isolation of target proteins by closing all valve sets; (e) further separation of isolated proteins. Reprinted with permission from Wang *et al.*<sup>41</sup> Copyright 2004 American Chemical Society.

such as PDMS. The valves have been shown to pump, restrict, and control flow within microfluidic devices with a high degree of repeatability and precision.<sup>93,94</sup> The elastomeric material forms reversible bonds through van der Waals forces against itself or the glass substrate. These reversible bonds are able to withstand pressures on the order of 100 kPa without failure.<sup>95–97</sup> However, within PDMS, heat is not dissipated as efficiently as within glass devices.<sup>39</sup> PDMS also exhibits some natural fluorescence properties which reduce the sensitivity of on-chip fluorescence detections.<sup>98</sup> PDMS and polycarbonate both have an additional advantage in that fabrication of multiple devices is relatively easy once a master mold has been created – by allowing the PDMS to set over a lithographed template or through hot embossing in the case of a polycarbonate substrate.<sup>58,99</sup> By controlling the pressures across elastomer valves, the Han group was able to electrically and fluidically isolate buffer and sample in their IEF-CE separations. Isolation allowed sample transfer with a minimum dead volume at the interface valve. Fig. 4 illustrates the valve actuation sequence which allowed loading of sample and all buffer solutions followed by two modes of separation.

Li *et al.* integrated denaturing IEF and SDS electrophoresis in a microfluidic channel network fabricated in polycarbonate and demonstrated the importance of separation media.<sup>80</sup> In Fig. 5, the authors used different separation media in each dimension. The reduced bandwidth is attributable to an electrokinetic and/or physical stacking effect at the IEF-gel interface, which increased the *SR* of the system. A peak capacity of  $\sim 1700$  was achieved within a footprint of 2 cm  $\times$  3 cm with capacities of approximately 10 and 170 for the IEF and CE separations, respectively. Heart cutting methods work especially well with microfluidic devices for IEF-CE, as IEF focused protein bands remain immobilized once the bands have reached their respective isoelectric points and therefore, many of the technical challenges that come with sampling a migrating analyte peak can be avoided.

Kohlheyer *et al.* performed two modes of separation on a microfabricated device without capillary IEF or CE, by fabricating a device that can perform both free flow electrophoresis and isoelectric focusing.<sup>100</sup> The free flow electrophoresis technique allows fine control over the position of a sample stream within a microfluidic device by sandwiching the sample flow between two sheath flow streams, which allows real time separation, sample monitoring and distribution.<sup>101,102</sup> The micro-device was fabricated from glass and used a photopolymerizable material as a membrane to resist pressure driven flow while allowing for ion transport. The membrane acts as a “salt bridge” providing hydrodynamic resistance without high electrical resistance – which reduced the voltage necessary to perform separations.

### Alternative separation strategies

While most of the pioneering work in developing microfluidic devices for multidimensional separations have utilized MEKC-CE or IEF-CE strategies, other modes of separation have also been combined on-chip. Some of these alternatives include electrochromatography, isotachopheresis, and temperature gradient gel electrophoresis. In electrochromatography, an electric field gradient is superimposed upon a stationary phase used for size exclusion chromatography. Using these two mechanisms, electrochromatography is utilized primarily for separation of large biomolecules. Gottschlich *et al.* dealt with the challenge of “racetrack” effect band broadening by utilizing a spiral channel geometry.<sup>42</sup> In this combined open channel electrochromatography (OCEC)-electrophoresis glass microchip, a long spiral OCEC channel design helped reduce band dispersion by maintaining a large radius of curvature (Fig. 6). Within the long spiral channel, a  $C_{18}$  stationary phase coating was uniformly applied, while the orthogonal channel for CE was left uncoated. An estimated peak capacity of  $\sim 150$  was achieved

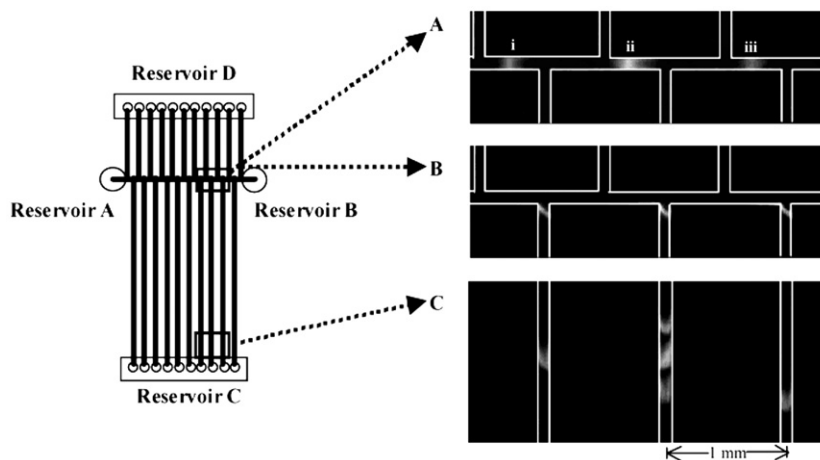


**Fig. 5** Fluorescence images demonstrate the 2D separation of five model proteins when utilizing multiple separation media within a single microfluidic device. (A) Non-native IEF in the horizontal channel with focusing order of (i) actin, (ii) bovine serum albumin, ovalbumin, and trypsin inhibitor, and (iii) parvalbumin from left to right; (B) electrokinetic transfer of focused proteins; (C) SDS gel electrophoresis. Images were captured at 90 s following the initiation of IEF or SDS gel electrophoresis separations. These were obtained using either green fluorescence of protein-fluorescein conjugates in IEF or red fluorescence of Sypro Red-labeled proteins during electrokinetic transfer and size-based separation. Reprinted with permission from Li *et al.*<sup>80</sup> Copyright 2004 American Chemical Society.

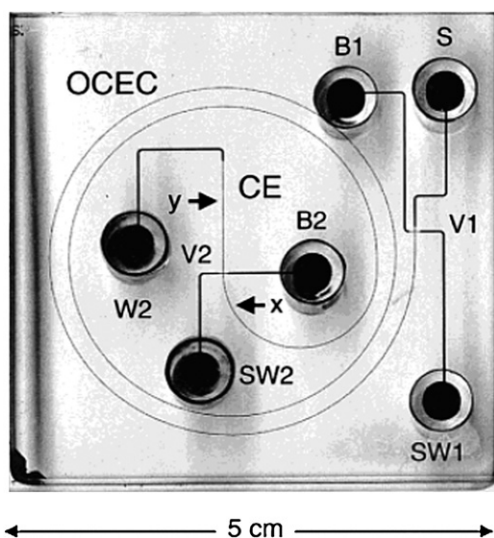


**Fig. 6** An image of the OCEC-CE device from Gottschlich *et al.*, demonstrates a large radius of curvature to minimize band broadening. The separation channel for the first dimension (OCEC) extends from the first valve V1 to the second valve V2. The second dimension (CE) extends from the second valve V2 to the detection point *y*. Sample (S), buffer 1 and 2 (B1, B2), sample waste 1 and 2 (SW1, SW2), and waste (W) reservoirs are positioned at the terminal of each channel. Arrows indicate the detection points in the OCEC channel (*x*) and CE channel (*y*). Channels and reservoirs are filled with black ink for contrast. Reprinted with permission from Gottschlich *et al.*<sup>42</sup> Copyright 2001 American Chemical Society.

for the 2D system, with a peak capacity of 30 in the first dimension and 5 in the second. Sample injection and sampling rates at the channel intersections were programmed, so that an estimated 9% of the total effluent from the first dimension was analyzed in the second (CE) dimension.

Slentz *et al.* coupled functional metal affinity chromatography with reverse-phase capillary electrochromatography in a chip.<sup>103</sup> The device was able to demonstrate three dimensions of on-chip chromatography with tryptic digestion of a protein followed by Copper(II)-immobilized metal affinity chromatography [Cu(II)-IMAC], affinity selection of histidine-containing peptides and reverse-phase chromatography of those selected peptides. Utilizing fluorescein isothiocyanate-labeled bovine serum albumin as a model protein, each stage of the device was validated with separations occurring on the order of minutes. Cu(II)-IMAC was conducted in a PDMS channel. Microfabricated frits were used within the device for multiple functions; to retain immobilized trypsin in one region of the device, to load Cu(II) in another region, and to maintain a constant path length and cross sectional area for particle transport. After the Cu(II)-IMAC process, selected peptides were eluted through a co-located monolithic support structure, modified with acrylamido-2-methylpropanesulfonic acid for reversed-phase separation.

Isotachopheresis relies on introducing a sample between a fast leading electrolyte and a slow terminating electrolyte with different electrical properties to achieve physical separation of analyte through equilibration under an applied electric potential. In microfluidic devices, ITP has been mainly employed as a preparative enrichment process prior to electrophoresis.<sup>104–106</sup>

In this manner, Jung *et al.* demonstrated the separation and detection of fluorophores in starting concentrations of  $\sim 100$  aM.<sup>105</sup> ITP within a microfluidic format has also been developed in great detail by the Kaniansky group,<sup>107–111</sup> including a combined ITP-CE chip in PMMA reported by Ōlvecká *et al.*<sup>112</sup> Here, the ITP enrichment and CE separation modes were performed along the same linear pathway (ITP followed by CE within the same capillary). The device was also hydrodynamically enclosed in the sense that once the necessary channels had been filled, peristaltic micropumps acted as valves to close the corresponding inlets, which improved the reproducibility of protein migration patterns within the device. The ITP-CE device also utilized a conductivity detector, bypassing the labeling steps required in fluorescence detection strategies.

Although not comprised of orthogonal modes of separation, the Ivory group reported on a PDMS device that was capable of multistage IEF.<sup>113</sup> By using a set of intersecting channels, the multi-stage IEF analysis achieved significantly higher resolutions by bringing focused proteins into second and third stages of separation with increasingly higher electric fields and shallower pH gradients. High viscosity methylcellulose solutions in the IEF channels improved performance. Similarly, Tsai *et al.* have reported on a method that was capable of employing two different modes of CE (with and without SDS treatment) on the same borosilicate glass microchip.<sup>55</sup> As demonstrated by the authors, performing electrophoretic separations on native and SDS-denatured proteins resulted in an increased degree of resolution over any single mode of CE. The coupling of two forms of electrophoresis presents the potential to increase the interrogative capacity of existing multidimensional separation systems which utilize on-chip CE.

While most of the devices presented in this review have detailed microfluidic systems intended for proteomic applications, other multidimensional separation techniques used for the analysis of metabolites and oligomers may find great potential in on-chip integration. Buch *et al.* presented promising work regarding denaturing gradient-based two-dimensional gene mutation scanning on a microfluidic format.<sup>114,115</sup> The technique utilized polymerase chain reaction (PCR) amplification in conjunction with a set of carefully programmed thermal and

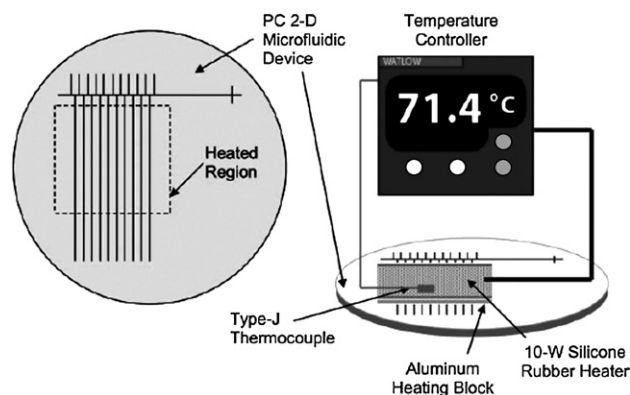


**Fig. 7** Illustration of the temporal temperature control set-up for on-chip denaturing gradient-based two-dimensional gene mutation scanning from Buch *et al.*<sup>115</sup> Reproduced by permission of the Royal Society of Chemistry.

chemical gradients as a way to detect DNA mutations within individuals.<sup>116–118</sup> The assay was translated onto a polycarbonate chip to make the process more efficient and low cost. In this method, DNA fragments were resolved on the basis of size *via* electrophoresis and base pair sequence through the comparison of predictive melting points. A critical component in the microfluidic system was the integrated heater and thermal sensor arrangement using an external control system through which the requisite temperature gradients were established (Fig. 7). Sequence identification was made possible through the use of a fluorescent label (YOYO-1) which was tagged to three PCR products of varying base pair length.

## 4. Critical challenges & future trends

### Shrewd choice of separation modules

Selection of orthogonal separation mechanisms is essential to optimize protein information extraction from a complex sample using any multidimensional system. This choice of separation mechanisms is influenced by the strong body of literature that has been developed to support slab gel and capillary-based separations. These existing separation mechanisms may often also involve coupling with MS, which allows previously unknown proteins to be identified based on an MS fingerprint.<sup>18,21,23,25,33,119</sup> To maximize effectiveness for proteomic discovery research, microchip-based separation techniques should also become MS-compatible.<sup>120</sup> The integration and application of microchip separation systems with various forms of MS has been demonstrated in several devices and covered in greater depth within other reviews.<sup>20,121–123</sup>

The performance (*i.e.*, *SR*, signal-to-noise, peak capacity) of a total system is also critically affected by sampling rate and transfer performance between successive dimensions. Separation processes can suffer if dispersion occurs during sample injection, if the sampling rate has not been optimized or if orthogonality is compromised.<sup>124</sup> The performance of each independent separation dimension is also important, and modifications to each dimension can result in overall system performance enhancement. For example, in published studies with devices for MEKC-CE, the Ramsey group was able to boost their reported capacity from the range of 500–1000 up to 4200 by implementing changes such as asymmetrically tapered turns, altered channel dimensions and optimized parameters for electric field strength and sampling.

Lastly, conventional chromatographic separation columns are quite flexible, owing to compatibility with hardware including multiple ports, pumps, and valves that allow introduction of different phase conditions in a variety of programmable sequences. Microfluidic fabrication techniques can be used to produce complex channel geometries with multiple channels and access points. To achieve comparable versatility to their column based counterparts, microfluidic devices are being integrated with flow control functionality including elastomer valves, polymeric features, and channels with varied fluidic resistance. Though the advantages of adapting multidimensional separations onto a microfluidic format are well documented, gas chromatography, and ion exchange chromatography are some of the common modes of separation that have had difficulty in

making the on-chip transition. HPLC is another valuable tool in the analysis of metabolites and oligomers that has only recently become integrated in a microfluidic format due to the logistical challenges of high operating pressure requirements.<sup>125–128</sup> Thus, much of the promise of on-chip multidimensional separation has yet to be fully realized. While the majority of work published deals with device validation, most proteomic research with clinical or pharmaceutical relevance which utilizes a multidimensional separation strategy continues within glass capillary, gel and chromatographic column forms.<sup>18,23,25,33,119,129</sup>

### Development of effective means to combine unit separations

Separation efficiency is not only influenced by sample leakage, but also by the method of injection into the second dimension. Debate exists regarding whether time-multiplexed or spatially multiplexed separations are able to provide more information about a given sample. Thoughtful work has been performed from both perspectives<sup>44,130–133</sup> with the goal of establishing uniform and repeatable techniques that avoid dispersive loss of sample. Approaches include computational simulations and analogous circuit analyses to ensure uniform electric field distribution and optimum geometric ratios at channel intersections.<sup>134,135</sup> Automated and programmable sample transfer in capillary and microfluidic formats offers significant potential advantages in reproducibility when compared to existing manual transfer processes for slab gels (*i.e.*, in transfer to MS). However, whether more information is gained through a serial analysis or a parallel analysis depends on the mode of separation (if it involves the sampling of a transient signal from a migrating peak) and upon the number of cross channels within the device that are available for sampling. Optimization of the size or arrangement of orthogonal channels can increase peak capacity and *SR*. Schemes that do not sample all fluid volumes from the full first dimension are effectively diminishing the peak capacity of that first separation and the final total peak capacity of the 2D system. For example, in the micro-DIGE analyzer,<sup>82</sup> an array of 20 radially oriented microchannels could be increased to a space-constrained limit of 50 microchannels. The larger number of second dimension channels would improve the resolution of the system by decreasing the spacing between each neighboring parallel channel.

In another approach, Li *et al.* employed a staggered (multiple-T) configuration so that the entire contents of the first dimension IEF channel were transferred to the second dimensional array in a single step.<sup>80</sup> The staggered-T geometry facilitates electrokinetic access to the entire IEF channel length. Further, the method was demonstrated to reduce band broadening that occurs during sample transfer (see Fig. 5). Yang and colleagues have recently provided further insight into the problem of electrokinetic sample transfer by proposing a dramatic redesign of the channel intersections, angling them at 45° rather than at perpendicular angles.<sup>133</sup> The geometric alteration was then coupled with additional channels for performing optimized back-biasing of the separation process. By programming a bias voltage at channels adjacent to the sample inlet and waste reservoirs, one can electrokinetically exclude excess sample from the injection zone to reduce leakage and influence sample transfer. In numerical simulation and in validation studies using fluorescence

indicators, the combination of strategies resulted in significantly smaller and more uniform field-induced plug formation in the second dimension.

These changes were implemented in a recent paper from the same group describing a 2-D PAGE microchip device in PMMA which also integrated the use of *in situ* polyacrylamide gel plugs and discontinuous buffer systems.<sup>136</sup> Not only do the gel plugs inhibit bulk flow and aid in fluid isolation, but they can also serve as reservoirs for the application of reagents such as SDS towards the analyte. A discontinuous buffer system was shown to enable an ITP stacking effect which enhances the SNR and the peak capacity for the SDS-treated CE separation when compared against electropherograms obtained from the same chip and a uniform buffer. The group also compared the results from different chips containing either 10 or 20 cross channels for CE and found that an increase in the number of sampling channels revealed a more complex pattern of peaks, especially at the extreme ends of the pH range due to the higher sampling resolution. Using an analysis of fluorescently labeled *E. coli* cell lysate (among other proteins) as a model, a peak capacity of approximately 2880 was achieved with capacities of 144 and 20 in the CE and IEF dimensions, respectively.

In the system presented by Rocklin *et al.*,<sup>45</sup> approximately 10% of the effluent from the first dimension is sampled as a comprehensive strategy is employed. However, the availability of proteomic information is not only dependent on the fraction of total effluent that can be transferred, but also upon the rate at which peaks can be sampled. With a higher sampling rate, more corresponding information from each band in the first dimension can then be introduced into the second dimensional analysis. In a 2003 paper published by the same group, the length of an MEKC separation channel was increased to 196 mm from 69 mm, and an overlapping set of analysis times was used to maximize sampling frequency and provide maximum throughput for the CE separation.<sup>44</sup> Timing cycles were based upon the difference between the fastest and slowest migrating components of the analyte and similarly, the applied field strength was tuned to provide the highest possible *SR* and efficiency for the application. With these changes, Ramsey *et al.*<sup>44</sup> were able to demonstrate a 3-fold increase in sampling rate and a peak capacity that was almost an order of magnitude greater than those of previous devices ( $\sim 110$  MEKC  $\times$   $\sim 38$  CE).

### System optimization

While *SR* is important, the repeatability of any measurement system is an essential factor and the complexity of these particular analytical systems makes achieving reproducibility a challenge.<sup>54,81</sup> Multidimensional systems are inherently complex; including at least two different chemical systems for separation and multiple channels for analysis, as well as hardware for timing of separations and sampling. Low sample injection dispersion during the primary injection (with the exception of focusing methods such as IEF) and subsequent sampling injections plays an important role. Using a modular miniature gel system, Demianova *et al.*<sup>37</sup> examined the repeatability of 2D measurements in microfluidic IEF-CE by recording the pI and molecular weight of each resolved protein. Over three runs, the average variation in migration distance for each species from gel-to-gel

was 6.2% ( $\pm 0.9\%$ ) with an average pI variation of 2.5% ( $\pm 0.6\%$ ), which is comparable to results from the commercially available 2D slab gel PhastSystem.<sup>23</sup>

In the multidimensional system presented by Emrich *et al.*, the reproducibility of peak elution patterns and electrophoretic current was improved by including a 7M urea solution in the electrophoresis run buffer and decreasing the field strength of the CE separation to minimize band distortion.<sup>82</sup> The addition of urea may have resulted in improved reproducibility because of an increase in protein solubility. In the end, samples still exhibited a small run-to-run variation, possibly due to a pH gradient compression in the separation channel. Similarly, Liu and colleagues examined peak elution times after implementing *in situ* photopolymerized gel plugs as hydrodynamic flow control elements, which resulted in an average variation of 4.1%.<sup>81</sup> The variation value was taken from the average of 11 resolved peaks, and compares favorably with the repeatability of conventional 2D slab gel PAGE.<sup>137</sup> Within the hydrodynamically closed ITP-CE device presented by Ölvecká *et al.*, variation in protein migration times was even lower – with relative standard deviations of 0.5% ( $n = 7$ ).<sup>112</sup>

### Development of sophisticated detection & data reduction systems

Integration of multiple steps has been implemented in commercially available 2D PAGE systems.<sup>138,139</sup> That said, integrated labeling (staining) of analytes is typically a time-consuming step requiring manual intervention. The majority of microdevices described in this review employed off-chip labeling and, consequently, did not take advantage of significant additional time and intervention requirements. Integration of on-chip staining, as demonstrated previously<sup>140</sup> could lead to a major reduction of the total time necessary to perform and analyze a multidimensional separation. Incomplete degrees of labeling may also be a significant source of measurement variability, so an efficient on-chip labeling process would likely contribute to improvements in system repeatability as well. The vast majority of the microdevices surveyed within this review have analyzed simple mixtures comprised of a few known samples. Using fully characterized biological standards is an excellent way of performing device validation. In the future however, it will be imperative for emerging device technologies to confront the technical challenges of preparing and analyzing complex, biologically relevant samples whose composition may be unknown. A limited number of studies have focused on this concern through the analysis of tryptically digested protein samples<sup>44,45,103</sup> or cell and tissue lysates.<sup>40,81,82</sup> In one case, Emrich *et al.* were able to use their on-chip system for the differential expression protein profiling of *E. Coli*.<sup>82</sup> In another example, Usui and colleagues have reported a chip-based system for 2D CE-IEF that was able to analyze extracted proteins from mouse brain tissue with an *SR* that was greater than that of a commercially available mini-gel system.<sup>40</sup>

For the sake of comparison with traditional 2D slab gels, researchers typically reconstruct two-dimensional gel-like plots from the electropherograms obtained during a multidimensional microchip separation.<sup>43</sup> Much room for improvement exists in data visualization, interpretation, and implementation of well established standards for image and data analysis of 2D

**Table 1** Summary of Microfluidic Devices for Multidimensional Separation and Analysis

Modes of Separation	Authors	Separation/Analysis Time	Year	Capacity	Notes	
MEKC-CE	Rocklin <i>et al.</i>	<10 mins	2000	~500–1000	One of the first instances of on-chip 2D separations	
	Ramsey <i>et al.</i>	<15 mins	2003	~4200	Asymmetrically tapered turns	
IEF-CE	Shadpour and Soper	~12 mins	2006	~1000	CE was followed by MEKC	
	Chen <i>et al.</i>	<10 mins	2002		Modular system	
	Herr <i>et al.</i>	estimated ~ 1h for total analysis	2003	~1300	First instance of on-chip, microfluidic serial IEF-CE	
	Griebel <i>et al.</i>	1.5 hours	2004		Modular IPG strip	
	Li <i>et al.</i>	<10 mins	2004	~1700	Demonstrated single and multiple separation media	
	Wang <i>et al.</i>	20 mins	2004		PDMS valves for channel isolation	
	Tsai <i>et al.</i>	~14 mins	2004		Air gap capillary	
	Usui <i>et al.</i>	< 1hour (20 mins for IEF)	2006		Minigel system	
	Das <i>et al.</i>	<10 minutes	2007		Photopolymerized <i>in situ</i> plugs	
	Demianova <i>et al.</i>	~80 minutes	2007		Modular minigel	
CEC-CE	Gottschlich <i>et al.</i>	13 mins	2001	~150	C18 stationary phase	
	Slentz <i>et al.</i>	13 mins	2003	~150	On-chip tryptic digestion followed by 3D chromatography	
	ITP-CE	Ölvecká <i>et al.</i>	~12 mins	2004		One of the first demonstrations of 2D on-chip ITP-CE
		IEF-FFE	Kohlheyser <i>et al.</i>	Continuous flow	2005	Real time flow monitoring
			CE-TGGE	Buch <i>et al.</i>	~5 min	2005
	Emrich <i>et al.</i>		2007	~48 for IEF	Passive microfluidic interface	
	Liu <i>et al.</i>	<10 mins total	2008		Polyacrylamide gel plugs	
	Yang <i>et al.</i>	~15 mins	2009	~2880	gel plugs and discontinuous buffers integrated with angled IEF channels and backbiasing	

separations.<sup>141–143</sup> A standardized set of software tools or algorithms for data processing of multidimensional separations similar to those available for researchers working in shotgun proteomics would serve as a valuable collective asset. Such facile and intuitive data presentation and manipulation tools could be especially important for those working in the field of biomarker validation. Through analysis of increasingly complex and biologically relevant samples, investigators will gain a greater comprehension of assay performance required for microfluidic devices. For example, the further development of integrated sample preparation (*e.g.*, on-chip affinity selection mechanisms) could certainly play an important role in this respect. Various innovations to address these issues share the goal of achieving levels of system capacity, sensitivity and resolution that are comparable to, if not better than the current benchmark standards for multidimensional analysis (Table 1). We see multidimensional assay developers tackling challenging and complex applications as a way to drive the multidimensional assay microtechnology beyond validation, and into full-scale proteomic discovery studies and a capacity for enabling generations of meaningful biological hypotheses.

## Acknowledgements

The authors thank Dr. Joshua Molho for critical comments. The authors also acknowledge Ms. Lavanya Wusirika and Ms. Zohora Iqbal for assistance with manuscript preparation. This work was supported by a National Science Foundation Graduate Research Fellowship to S.T., a University of California Regents' Junior Faculty Fellowship to A.E.H., and the University of California, Berkeley.

## References

- O. Smithies and M. D. Poulik, *Nature*, 1956, **177**, 1033.
- J. C. Giddings, *Anal. Chem.*, 1984, **56**, 1258A–1270A.
- M. M. Bushey and J. W. Jorgenson, *Anal. Chem.*, 1990, **62**, 161–167.
- J. M. Busnel, N. Lion and H. H. Girault, *Anal. Chem.*, 2007, **79**, 5949–5955.
- R. Cabrera, P. Zhelyazkova, L. Galvis and M. Fernandez-Lahore, *J. Sep. Sci.*, 2008, **31**, 2500–2510.
- J. Chen, B. M. Balgley, D. L. DeVoe and C. S. Lee, *Anal. Chem.*, 2003, **75**, 3145–3152.
- D. Mohan and C. S. Lee, *Electrophoresis*, 2002, **23**, 3160–3167.
- P. H. O'Farrell, *J. Biol. Chem.*, 1975, **250**, 4007–4021.
- M. Zhang and Z. El Rassi, *J. Proteome Res.*, 2006, **5**, 2001–2008.
- R. Aebersold, D. Figeys, S. Gygi, G. Corthals, P. Haynes, B. Rist, J. Sherman, Y. Zhang and D. Goodlett, *J. Protein Chem.*, 1998, **17**, 533–535.
- L. Mondello, P. Q. Tranchida, P. Dugo and G. Dugo, *Mass Spectrom. Rev.*, 2008, **27**, 101–124.
- C. E. Costello, *Biophys. Chem.*, 1997, **68**, 173–188.
- R. Bharadwaj, J. G. Santiago and B. Mohammadi, *Electrophoresis*, 2002, **23**, 2729–2744.
- L. R. Snyder and J. W. Dolan, *High-performance gradient elution: the practical application of the linear-solvent-strength model*, Wiley-Interscience, Hoboken, N.J., 2007.
- J. C. Giddings, *Unified Separation Science*, Wiley-Interscience, 1991.
- A. W. Moore, Jr. and J. W. Jorgenson, *Anal. Chem.*, 1995, **67**, 3456–3463.
- H. Y. Tang, N. Ali-Khan, L. A. Echan, N. Levenkova, J. J. Rux and D. W. Speicher, *Proteomics*, 2005, **5**, 3329–3342.
- J. Astorga-Wells, S. Tryggvason, S. Vollmer, G. Alvelius, C. Palmberg and H. Jornvall, *Anal. Biochem.*, 2008, **381**, 33–42.
- M. L. Fournier, J. M. Gilmore, S. A. Martin-Brown and M. P. Washburn, *Chem. Rev.*, 2007, **107**, 3654–3686.
- R. Tomas, K. Kleparnik and F. Foret, *J. Sep. Sci.*, 2008, **31**, 1964–1979.
- M. Vollmer, P. Horth, G. Rozing, Y. Coute, R. Grimm, D. Hochstrasser and J. C. Sanchez, *J. Sep. Sci.*, 2006, **29**, 499–509.
- Y. Wagner, A. Sickmann, H. E. Meyer and G. Daum, *J. Am. Soc. Mass Spectrom.*, 2003, **14**, 1003–1011.

- 23 A. Lapin and W. Feigl, *Electrophoresis*, 1991, **12**, 472–478.
- 24 S. E. Ong and A. Pandey, *Biomol Eng*, 2001, **18**, 195–205.
- 25 L. Pattini, S. Mazzara, A. Conti, S. Iannaccone, S. Cerutti and M. Alessio, *Exp Biol Med (Maywood)*, 2008, **233**, 483–491.
- 26 E. Hagemeyer, K. Kemper, K. S. Boos and E. Schlimme, *J Chromatogr*, 1983, **282**, 663–669.
- 27 A. P. Kohne and T. Welsch, *J Chromatogr A*, 1999, **845**, 463–469.
- 28 P. O'Connor, S. Fremont, J. Schneider, H. Dowty, M. Jaeger, G. Talaska and D. Warshawsky, *J Chromatogr B Biomed Sci Appl*, 1997, **700**, 49–57.
- 29 N. Tanaka, H. Kimura, D. Tokuda, K. Hosoya, T. Ikegami, N. Ishizuka, H. Minakuchi, K. Nakanishi, Y. Shintani, M. Furuno and K. Cabrera, *Anal Chem*, 2004, **76**, 1273–1281.
- 30 R. L. Moritz, H. Ji, F. Schutz, L. M. Connolly, E. A. Kapp, T. P. Speed and R. J. Simpson, *Anal Chem*, 2004, **76**, 4811–4824.
- 31 M. Baranyi, E. Milusheva, E. S. Vizi and B. Sperlagh, *J Chromatogr A*, 2006, **1120**, 13–20.
- 32 G. Morovjan, B. Dalmadi-Kiss, I. Klebovich and E. Mincsovcis, *J Chromatogr Sci*, 2002, **40**, 603–608.
- 33 S. Uttenweiler-Joseph, S. Claverol, L. Sylvius, M. P. Bousquet-Dubouch, O. Burlet-Schiltz and B. Monsarrat, *Methods Mol Biol*, 2008, **484**, 111–130.
- 34 J. W. Cooper, Y. Wang and C. S. Lee, *Electrophoresis*, 2004, **25**, 3913–3926.
- 35 H. J. Issaq, K. C. Chan, G. M. Janini, T. P. Conrads and T. D. Veenstra, *J Chromatogr B Analyt Technol Biomed Life Sci*, 2005, **817**, 35–47.
- 36 I. Neverova and J. E. Van Eyk, *J Chromatogr B Analyt Technol Biomed Life Sci*, 2005, **815**, 51–63.
- 37 Z. Demianova, M. Shimmo, E. Poysa, S. Franssila and M. Baumann, *Electrophoresis*, 2007, **28**, 422–428.
- 38 A. Griebel, S. Rund, F. Schonfeld, W. Dorner, R. Konrad and S. Hardt, *Lab Chip*, 2004, **4**, 18–23.
- 39 X. Chen, H. Wu, C. Mao and G. M. Whitesides, *Anal Chem*, 2002, **74**, 1772–1778.
- 40 K. Usui, A. Hiratsuka, K. Shiseki, Y. Maruo, T. Matsushima, K. Takahashi, Y. Unuma, K. Sakairi, I. Namatame, Y. Ogawa and K. Yokoyama, *Electrophoresis*, 2006, **27**, 3635–3642.
- 41 Y. C. Wang, M. H. Choi and J. Han, *Anal Chem*, 2004, **76**, 4426–4431.
- 42 N. Gottschlich, S. C. Jacobson, C. T. Culbertson and J. M. Ramsey, *Anal Chem*, 2001, **73**, 2669–2674.
- 43 A. E. Herr, J. I. Molho, K. A. Drouvalakis, J. C. Mikkelsen, P. J. Utz, J. G. Santiago and T. W. Kenny, *Anal Chem*, 2003, **75**, 1180–1187.
- 44 J. D. Ramsey, S. C. Jacobson, C. T. Culbertson and J. M. Ramsey, *Anal Chem*, 2003, **75**, 3758–3764.
- 45 R. D. Rocklin, R. S. Ramsey and J. M. Ramsey, *Anal Chem*, 2000, **72**, 5244–5249.
- 46 H. Shadpour and S. A. Soper, *Anal Chem*, 2006, **78**, 3519–3527.
- 47 R. E. Murphy, M. R. Schure and J. P. Foley, *Anal Chem*, 1998, **70**, 1585–1594.
- 48 A. Pandey and M. Mann, *Nature*, 2000, **405**, 837–846.
- 49 T. Greibrokk, *J Sep Sci*, 2006, **29**, 479–480.
- 50 X. Yang, X. Zhang, A. Li, S. Zhu and Y. Huang, *Electrophoresis*, 2003, **24**, 1451–1457.
- 51 H. Becker, K. Lowack and A. Manz, *J. Micromech. Microeng.*, 1998, **8**, 24–28.
- 52 A. Hierlemann, O. Brand, C. Hagleitner and H. Baltes, *Proc. IEEE*, 2003, **91**, 839–863.
- 53 E. Verpoorte and N. F. De Rooij, *Proc. IEEE*, 2003, **91**, 930–953.
- 54 S. Tsai, M. Loughran and I. Karube, *J. Micromech. Microeng.*, 2004, **14**, 1693–1699.
- 55 S. W. Tsai, M. Loughran, H. Suzuki and I. Karube, *Electrophoresis*, 2004, **25**, 494–501.
- 56 C. G. Khan Malek, *Anal Bioanal Chem*, 2006, **385**, 1351–1361.
- 57 C. G. Khan Malek, *Anal Bioanal Chem*, 2006, **385**, 1362–1369.
- 58 L. E. Locascio, D. J. Ross, P. B. Howell and M. Gaitan, *Methods Mol Biol*, 2006, **339**, 37–46.
- 59 E. A. Waddell, *Methods Mol Biol*, 2006, **321**, 27–38.
- 60 H. Becker and C. Gartner, *Anal Bioanal Chem*, 2008, **390**, 89–111.
- 61 J. S. Rossier, C. Vollet, A. Carnal, G. Lagger, V. Gobry, H. H. Girault, P. Michel and F. Reymond, *Lab Chip*, 2002, **2**, 145–150.
- 62 M. Hecke, W. Bacher and K. D. Muller, *Microsystem Technologies*, 1998, **4**, 122–124.
- 63 Y. J. Juang, L. J. Lee and K. W. Koelling, *Polymer Engineering and Science*, 2002, **42**, 539–550.
- 64 J. Giboz, T. Copponnex and P. Mele, *Journal of Micromechanics and Microengineering*, 2007, **17**, R96–R109.
- 65 J. Liu and M. L. Lee, *Electrophoresis*, 2006, **27**, 3533–3546.
- 66 S. Terabe, K. Otsuka, K. Ichikawa, A. Tsuchiya and T. Ando, *Anal Chem*, 1984, **56**, 111–113.
- 67 J. P. Kutter, S. C. Jacobson and J. M. Ramsey, *Anal Chem*, 1997, **69**, 5165–5171.
- 68 A. W. Moore, Jr., S. C. Jacobson and J. M. Ramsey, *Anal Chem*, 1995, **67**, 4185–4189.
- 69 F. von Heeren, E. Verpoorte, A. Manz and W. Thormann, *Anal Chem*, 1996, **68**, 2044–2053.
- 70 C. T. Culbertson, S. C. Jacobson and J. M. Ramsey, *Anal Chem*, 1998, **70**, 3781–3789.
- 71 S. C. Jacobson, R. Hergenroder, L. B. Koutny, R. J. Warmack and J. M. Ramsey, *Anal Chem*, 1994, **66**, 1107–1113.
- 72 J. I. Molho, A. E. Herr, B. P. Mosier, J. G. Santiago, T. W. Kenny, R. A. Brennen, G. B. Gordon and B. Mohammadi, *Anal Chem*, 2001, **73**, 1350–1360.
- 73 E. Zubritsky, *Anal Chem*, 2000, **72**, 687A–690A.
- 74 S. K. Griffiths and R. H. Nilson, *Anal Chem*, 2000, **72**, 5473–5482.
- 75 B. M. Paegel, L. D. Hutt, P. C. Simpson and R. A. Mathies, *Anal Chem*, 2000, **72**, 3030–3037.
- 76 C. T. Culbertson, S. C. Jacobson and J. M. Ramsey, *Anal Chem*, 2000, **72**, 5814–5819.
- 77 J. M. Hille, A. L. Freed and H. Watzig, *Electrophoresis*, 2001, **22**, 4035–4052.
- 78 G. H. W. Sanders and A. Manz, *Trends Anal. Chem.*, 2000, **19**, 364–378.
- 79 C. Das, J. Zhang, N. D. Denslow and Z. H. Fan, *Lab Chip*, 2007, **7**, 1806–1812.
- 80 Y. Li, J. S. Buch, F. Rosenberger, D. L. DeVoe and C. S. Lee, *Anal Chem*, 2004, **76**, 742–748.
- 81 J. Liu, S. Yang, C. S. Lee and D. L. DeVoe, *Electrophoresis*, 2008, **29**, 2241–2250.
- 82 C. A. Emrich, I. L. Medintz, W. K. Chu and R. A. Mathies, *Anal Chem*, 2007, **79**, 7360–7366.
- 83 C. H. Chen, H. Lin, S. K. Lele and J. G. Santiago, *Journal of Fluid Mechanics*, 2005, **524**, 263–303.
- 84 J. D. Posner and J. G. Santiago, *Journal of Fluid Mechanics*, 2006, **555**, 1–42.
- 85 C. Das, C. K. Fredrickson, Z. Xia and Z. H. Fan, *Sens. Actuators, A*, 2007, **134**, 271–277.
- 86 A. V. Hatch, A. E. Herr, D. J. Throckmorton, J. S. Brennan and A. K. Singh, *Anal Chem*, 2006, **78**, 4976–4984.
- 87 A. E. Herr, A. V. Hatch, D. J. Throckmorton, H. M. Tran, J. S. Brennan, W. V. Giannobile and A. K. Singh, *Proc Natl Acad Sci U S A*, 2007, **104**, 5268–5273.
- 88 A. E. Herr and A. K. Singh, *Anal Chem*, 2004, **76**, 4727–4733.
- 89 K. G. Olsen, D. J. Ross and M. J. Tarlov, *Anal Chem*, 2002, **74**, 1436–1441.
- 90 S. Song, A. K. Singh and B. J. Kirby, *Anal Chem*, 2004, **76**, 4589–4592.
- 91 S. Song, A. K. Singh, T. J. Sheppard and B. J. Kirby, *Anal Chem*, 2004, **76**, 2367–2373.
- 92 C. Yu, M. H. Davey, F. Svec and J. M. Frechet, *Anal Chem*, 2001, **73**, 5088–5096.
- 93 E. P. Kartalov, W. F. Anderson and A. Scherer, *J Nanosci Nanotechnol*, 2006, **6**, 2265–2277.
- 94 T. Thorsen, S. J. Maerkl and S. R. Quake, *Science*, 2002, **298**, 580–584.
- 95 J. Melin and S. R. Quake, *Annu Rev Biophys Biomol Struct*, 2007, **36**, 213–231.
- 96 A. M. Christensen, D. A. Chang-Yen and B. K. Gale, *J. Micromech. Microeng.*, 2005, **15**, 928–934.
- 97 M. A. Unger, H. P. Chou, T. Thorsen, A. Scherer and S. R. Quake, *Science*, 2000, **288**, 113–116.
- 98 A. Piruska, I. Nikcevic, S. H. Lee, C. Ahn, W. R. Heineman, P. A. Limbach and C. J. Seliskar, *Lab Chip*, 2005, **5**, 1348–1354.
- 99 J. M. Ng, I. Gitlin, A. D. Stroock and G. M. Whitesides, *Electrophoresis*, 2002, **23**, 3461–3473.
- 100 D. Kohlheyer, G. A. Besselink, S. Schlautmann and R. B. Schasfoort, *Lab Chip*, 2006, **6**, 374–380.
- 101 D. E. Raymond, A. Manz and H. M. Widmer, *Anal Chem*, 1994, **66**, 2858–2965.

- 102 D. E. Raymond, A. Manz and H. M. Widmer, *Anal Chem*, 1996, **68**, 2515–2522.
- 103 B. E. Slentz, N. A. Penner and F. E. Regnier, *J Chromatogr A*, 2003, **984**, 97–107.
- 104 B. Jung, R. Bharadwaj and J. G. Santiago, *Anal Chem*, 2006, **78**, 2319–2327.
- 105 B. Jung, Y. Zhu and J. G. Santiago, *Anal Chem*, 2007, **79**, 345–349.
- 106 A. Wainright, S. J. Williams, G. Ciambro, Q. Xue, J. Wei and D. Harris, *J Chromatogr A*, 2002, **979**, 69–80.
- 107 R. Bodor, D. Kaniansky, M. Masar, K. Silleova and B. Stanislawski, *Electrophoresis*, 2002, **23**, 3630–3637.
- 108 R. Bodor, V. Madajova, D. Kaniansky, M. Masar, M. Johnck and B. Stanislawski, *J Chromatogr A*, 2001, **916**, 155–165.
- 109 D. Kaniansky, M. Masar, J. Bielikova, F. Ivanyi, F. Eisenbeiss, B. Stanislawski, B. Grass, A. Neyer and M. Johnck, *Anal Chem*, 2000, **72**, 3596–3604.
- 110 D. Kaniansky, M. Masar, R. Bodor, M. Zuborova, E. Olvecka, M. Johnck and B. Stanislawski, *Electrophoresis*, 2003, **24**, 2208–2227.
- 111 M. Masar, D. Kaniansky, R. Bodor, M. Johnck and B. Stanislawski, *J Chromatogr A*, 2001, **916**, 167–174.
- 112 E. Olvecka, D. Kaniansky, B. Pollak and B. Stanislawski, *Electrophoresis*, 2004, **25**, 3865–3874.
- 113 H. Cui, K. Horiuchi, P. Dutta and C. F. Ivory, *Anal Chem*, 2005, **77**, 7878–7886.
- 114 J. S. Buch, C. Kimball, F. Rosenberger, W. E. Highsmith, Jr., D. L. DeVoe and C. S. Lee, *Anal Chem*, 2004, **76**, 874–881.
- 115 J. S. Buch, F. Rosenberger, W. E. Highsmith, Jr., C. Kimball, D. L. DeVoe and C. S. Lee, *Lab Chip*, 2005, **5**, 392–400.
- 116 N. J. van Orsouw, R. K. Dhanda, R. D. Rines, W. M. Smith, I. Sigalas, C. Eng and J. Vijg, *Nucleic Acids Res*, 1998, **26**, 2398–2406.
- 117 R. K. Dhanda, N. J. van Orsouw, I. Sigalas, C. Eng and J. Vijg, *Biotechniques*, 1998, **25**, 664–668, 670, 672–665.
- 118 R. D. Rines, N. J. van Orsouw, I. Sigalas, F. P. Li, C. Eng and J. Vijg, *Carcinogenesis*, 1998, **19**, 979–984.
- 119 X. Fang, L. Yang, W. Wang, T. Song, C. S. Lee, D. L. DeVoe and B. M. Balgley, *Anal Chem*, 2007, **79**, 5785–5792.
- 120 J. S. Mellors, A. G. Chambers, W. H. Henley and J. M. Ramsey, in *The Proceedings of the 12th International Conference on Miniaturized Systems for Chemistry and Life Sciences*, ed. L. E. Locascio, San Diego, CA, 2008.
- 121 D. L. DeVoe and C. S. Lee, in *Handbook of Capillary and Microchip Electrophoresis and Associated Microtechniques*, ed. J. P. Landers, CRC Press, Boca Raton, FL, 2007, pp. 1001–1012.
- 122 D. Figeys, S. P. Gygi, G. McKinnon and R. Aebersold, *Anal Chem*, 1998, **70**, 3728–3734.
- 123 G. E. Yue, M. G. Roper, E. D. Jeffery, C. J. Easley, C. Balchunas, J. P. Landers and J. P. Ferrance, *Lab Chip*, 2005, **5**, 619–627.
- 124 M. Gilar, P. Olivova, A. E. Daly and J. C. Gebler, *Anal Chem*, 2005, **77**, 6426–6434.
- 125 Y. Shintani, K. Hirako, M. Motokawa, Y. Takano, M. Furuno, H. Minakuchi and M. Ueda, *Anal Sci*, 2004, **20**, 1721–1723.
- 126 P. Sajonz, W. Schafer, X. Gong, S. Shultz, T. Rosner and C. J. Welch, *J Chromatogr A*, 2007, **1145**, 149–154.
- 127 J. Xie, Y. Miao, J. Shih, Y. C. Tai and T. D. Lee, *Anal Chem*, 2005, **77**, 6947–6953.
- 128 H. Yin and K. Killeen, *J Sep Sci*, 2007, **30**, 1427–1434.
- 129 A. Guttman, M. Varoglu and J. Khandurina, *Drug Discov Today*, 2004, **9**, 136–144.
- 130 J. P. Alarie, S. C. Jacobson and J. M. Ramsey, *Electrophoresis*, 2001, **22**, 312–317.
- 131 S. V. Ermakov, S. C. Jacobson and J. M. Ramsey, *Anal Chem*, 2000, **72**, 3512–3517.
- 132 L. M. Fu, R. J. Yang, G. B. Lee and H. H. Liu, *Anal Chem*, 2002, **74**, 5084–5091.
- 133 S. Yang, J. Liu and D. L. DeVoe, *Lab Chip*, 2008, **8**, 1145–1152.
- 134 M. A. Lerch, M. D. Hoffman and S. C. Jacobson, *Lab Chip*, 2008, **8**, 316–322.
- 135 M. A. Lerch and S. C. Jacobson, *Anal Chem*, 2007, **79**, 7485–7491.
- 136 S. Yang, J. Liu, C. S. Lee and D. L. DeVoe, *Lab Chip*, 2009.
- 137 A. Hiratsuka, H. Kinoshita, Y. Maruo, K. Takahashi, S. Akutsu, C. Hayashida, K. Sakairi, K. Usui, K. Shiseki, H. Inamochi, Y. Nakada, K. Yodoya, I. Namatame, Y. Unuma, M. Nakamura, K. Ueyama, Y. Ishii, K. Yano and K. Yokoyama, *Anal Chem*, 2007, **79**, 5730–5739.
- 138 M. Kramlova, T. I. Pristoupil, V. Fricova and J. Kraml, *J Chromatogr*, 1986, **367**, 443–445.
- 139 D. Hochstrasser, V. Augsburger, T. Pun, D. Weber, C. Pellegrini and A. F. Muller, *Clin Chem*, 1988, **34**, 166–170.
- 140 L. Bousse, S. Mouradian, A. Minalla, H. Yee, K. Williams and R. Dubrow, *Anal Chem*, 2001, **73**, 1207–1212.
- 141 J. E. Bandow, J. D. Baker, M. Berth, C. Painter, O. J. Sepulveda, K. A. Clark, I. Kilty and R. A. VanBogelen, *Proteomics*, 2008, **8**, 3030–3041.
- 142 M. Berth, F. M. Moser, M. Kolbe and J. Bernhardt, *Appl Microbiol Biotechnol*, 2007, **76**, 1223–1243.
- 143 R. Pedreschi, M. L. Hertog, S. C. Carpentier, J. Lammertyn, J. Robben, J. P. Noben, B. Panis, R. Swennen and B. M. Nicolai, *Proteomics*, 2008, **8**, 1371–1383.